

Experimental Model of the Interfacial Instability of Aluminium Reduction Cells

Alex Pedchenko¹, Sergei Molokov¹, Janis Priede¹, Alex Lukyanov², Peter J. Thomas³

¹Coventry University, Applied Mathematics Research Centre, UK

²University of Reading, UK

³University of Warwick, Fluid Dynamics Research Centre, UK

Abstract

We report on experimental model of magnetohydrodynamical instability of liquid metal pad occurring in Aluminium reduction cells. Developed room-temperature laboratory model uses simplified geometry of the cell, room-temperature liquid metal InGaSn to simulate liquid Aluminium and special anode construction, which allowed to eliminate the use of electrolyte in the experiment and to achieve generation of the instability. Experiment demonstrates rolling-pad instability wave propagating along the side walls of the cell, dependence of the wave amplitude on the cell current and background vertical magnetic field. Measurement techniques used in this study allowed to detect fluctuations of the melt boundary and distribution of the electric potential in the liquid metal during the wave propagation.

Introduction

Primary Aluminium is produced from alumina (bauxite ore) by electrolytic extraction (Hall-Héroult process) in shallow, few meters wide and >10 m long electrolysis cells ('pots') by passing an electric current of up to 500 kA through a mixture of alumina and cryolite (sodium aluminium fluoride). The electric current flows vertically down from the carbon anodes at the top of the cell to the carbon cathode at the bottom melting both alumina and cryolite.

As a result of very complex thermo-dynamical and electrochemical processes involving oxidation of carbon from anodes followed by CO₂ emissions and precipitation of the metallic Aluminium at the cathode, a two-fluid layer is formed. The fluid on top is an electrolyte with very poor electrical conductivity of $\sigma_c \approx 200 \text{ S/m}$ while the fluid below is a slightly heavier molten aluminium with high conductivity of $\sigma_m \approx 3 \cdot 10^6 \text{ S/m}$. Both are kept at about 950 °C.

The interface between the electrolyte and the liquid metal may become unstable to MHD waves if certain parameters of the process exceed thresholds which are discussed below. The key to the mechanism of instability, suggested first by Thornliif Sele [1], is the interaction of the horizontal component of the electric current within highly conducting aluminium layer with the vertical component of the background magnetic field generated by the bus bars supplying electric power to the cell. This produces horizontal Lorentz force which drives the liquid metal into sloshing motion. In the case of resonance between two sloshing components, instability grows and rotating interfacial wave is generated.

Up to now the most studies of the instabilities have been theoretical, see the review in [2], suggesting various mechanisms and flow models, but none of these models has been verified experimentally. Thus the necessity of low-temperature model of the instability involving non-aggressive fluids is essential.

Here we present a solution for experimental modelling, which eliminates the need for an electrolyte in the experiment and thus electrolysis altogether allowing to create a low-temperature model which reproduces Sele-type of instability. In this model the electrolyte is replaced by a system of 900 thin vertical steel rods connecting the anode plate and liquid metal. Since electric conductivity of such rods is much lower than the liquid metal one, this fulfils the electrodynamic feature of the electrolyte to conduct current vertically down into the liquid metal but at the same time eliminates all the problems related to the electrolysis.

The experimental model

The experimental cell depicted in Fig. 1 represents a container with square horizontal cross-section with dimensions of 30 × 30 cm. The cell with electrically insulating side walls and a stainless steel bottom was filled with a thin layer (1...5 cm) of

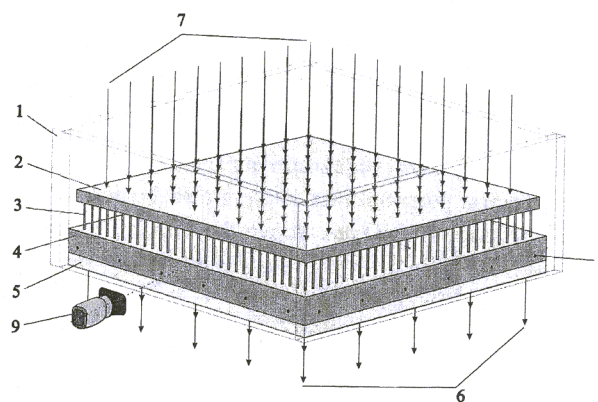


Fig.1 Sketch of the experimental model: 1 - Plexiglass side walls, 2 - copper anode plate, 3 - 900 stainless steel electrodes (2 mm diam.), 4 - liquid metal In-Ga-Sn, 5 - stainless steel cathode plate, 6 - cathode connecting wires (25 pcs.), 7 - anode current supplying wires (100 pcs.), 8 - potential probes, 9 - CCD camera for the melt interface position tracking.

room-temperature liquid metal alloy In-Ga-Sn, as a replacement of aluminium. The electric current was supplied to the metal pad from the anode, located on the top of the cell. It is a 15 cm thick copper plate with 900, 40 mm long, \varnothing 2 mm electrodes made of stainless steel, which were inserted into the bottom surface of the anode plate. The electrodes were distributed uniformly along the surface of the copper plate with a 10 mm pitch, and being directly immersed into the liquid metal with their tips, conducted the electric current between nearly equipotential anode plate and the liquid metal. The immersion depth of the electrodes could be varied by lowering or lifting the anode plate. The surface of liquid metal was free to move along the electrodes, in the gap with the anode plate. The effective conductivity of the system of such electrodes is 75 times lower than the one of the same height of liquid metal. The electrodynamic properties of the electrodes are similar to those of the electrolyte: if the liquid metal rises in some area of the cell, the resistance of the electrodes in that region reduces, causing higher current in that area of liquid metal and other way around for the melt areas with lowered height. In other words, the disturbance of the melt surface is driving non-homogeneity of the anode current, which enters the liquid metal and redistributes horizontally within the liquid metal layer before entering the electrically less conducting steel bottom. This is essentially the same mechanism of instability as known to occur in real cells.

The space between the anode plate and melt surface was filled with weak (~ 3%) alcohol and HCl solution to avoid liquid metal sticking to the side walls during sloshing, and to provide some cooling for the anode electrodes in the case of electric contact loss between some of the electrodes and the liquid metal. The second liquid, however, did not conduct electric current, but served to minimise density difference between both fluids.

Maximal anode current achievable in the experiment was 1.8 kA, which is much lower than the one of the real cells. However in the experiment were able to apply significantly higher background DC magnetic field (up to 20 times of the real cells). Vertical magnetic field was generated by two induction coils of quadratic shape (not shown in Fig. 2) surrounding the cell. The cell was placed in the gap between these two coils (Helmholtz configuration), in the region where magnetic field was nearly vertical with ~5% non-uniformity along the melt area and absolute value of up to 0.1T.

Measurement technique

To register the liquid metal surface oscillations two measurement techniques were used: (I) registration of the electric potential distribution along the liquid metal perimeter (Fig. 1, pos.8) and (II) tracking of the liquid metal interface position at some fixed point of the cell perimeter with video camera (Fig. 2, pos.9).

In the undisturbed state, distribution of the electric potential φ_0 in the liquid metal is stationary; it is formed by the anode current passing through the liquid metal layer. If some disturbance of the liquid metal interface is propagating in the cell with velocity \mathbf{v} under magnetic field \mathbf{B} , the electric potential perturbation $\varphi - \varphi_0$ is formed by local change in the resistance of the anode's electrodes φ_A and the electric field induced due to the motion of the melt $\mathbf{v} \times \mathbf{B}$, where \mathbf{v} is propagation velocity. The potential difference in the melt was measured between the center of the melt and its periphery. At such long distance between the electrodes and propagation velocity of the gravity wave, $\nabla(\mathbf{v} \times \mathbf{B}) \gg \varphi_A$, and essentially our potential measurements represent flow rate of the melt through the line connecting these two electrodes. Since the liquid metal height is changing in time along the perimeter of the cell due to wave propagation and assuming that propagation velocity and form of the wave are the same along the perimeter, the different flow rates measured at different points along the perimeter are proportional to the liquid metal height at these points.

24 electric potential probes were distributed uniformly along the perimeter of the cell and installed at the inner surface of the sidewalls 10 mm above the bottom. Instant values of the electric potential along the perimeter of the cell were recorded. Results of these measurements provided qualitative picture on the overall behaviour of the liquid metal surface at $\mathbf{B} = \text{const}$.

The second measurement technique used in the experiment (high-resolution video capture of the liquid metal height at the middle of the side wall - Fig. 1 pos.9) allowed to compare surface fluctuations' amplitude for different B_0 values. After digital post-processing of captured frames it was possible to obtain time-history of some point at the edge of the liquid metal surface. This data provided information on the amplitude, waveform, frequency and spectra of the oscillations.

Results

The procedure of the experiments was as follows: first, the anode was lowered for its electrodes to immerse in the liquid metal. Next, the anode current was switched on to the maximal value of 1.8 kA and, after that, vertical DC magnetic field was applied. If the value of B_0 is high enough to provide initial perturbation of the surface, the instability evolves rapidly. It manifests itself as a rotating interface of the liquid metal with counter-clockwise rotation direction (assuming

B points up and **I** - down). Switching direction of vertical magnetic field changes the direction of rotation. The height of the wave varies in a wide range of 3...50 mm rising with the anode current I_0 and magnetic field B_0 . Fig. 2 provides time-history of the measured electric potential map during the wave propagation reconstructed from the electric potential acquired along the perimeter of the cell. The rest of the surface is the result of interpolation. It represents the rotating surface with the local height (electric potential value) proportional to the height of the metal at that position. The obtained map of the potential correlates very well with visual observations of the liquid metal interface and its shape can be described by sum of two sinusoidal waves sloshing along both sidewalls.

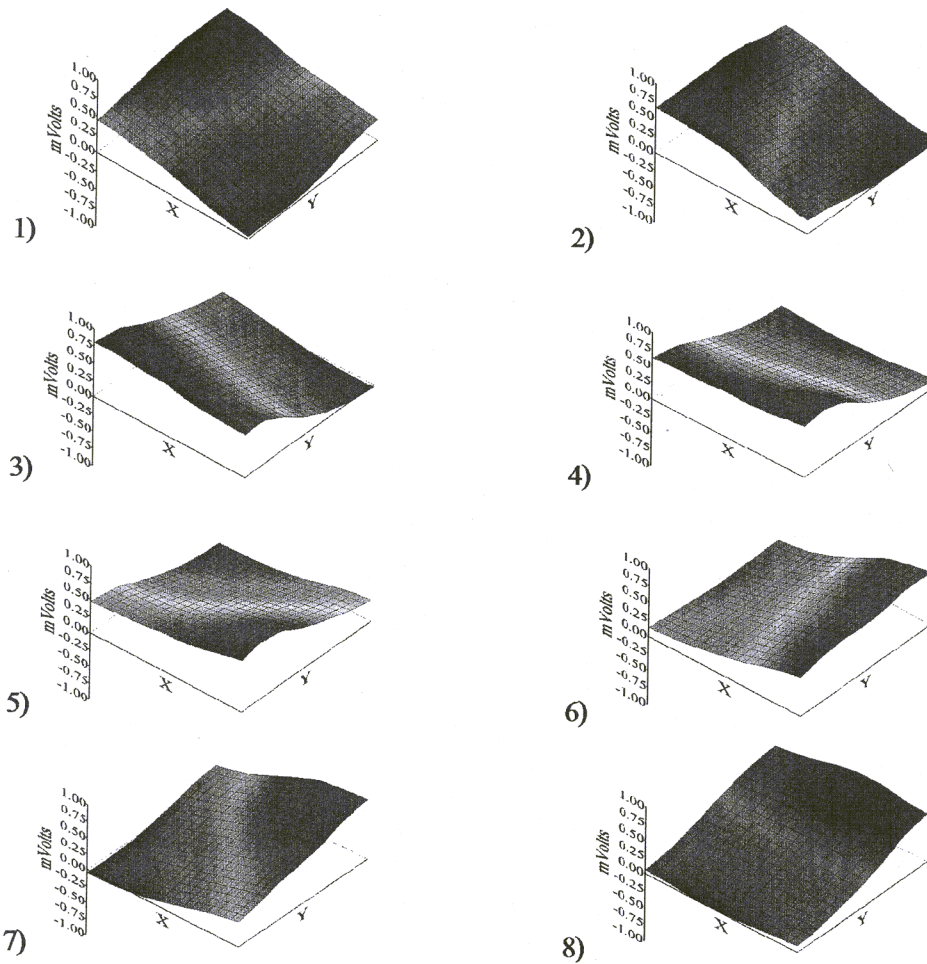


Fig. 2 Time-evolution of the electric potential in the liquid metal recorded with potential probes along the perimeter of the cell during propagation of instability wave. Here time interval between frames is 0.13 s; $I_0 = 80A$, $B_0 = 30 mT$, $h_0 = 2 cm$. The wave propagates counter-clockwise.

Frequency of the wave observed in the experiment varied with the thickness h_0 of the liquid metal layer in the range of 0.5...0.9 Hz ($h_0 = 10...45 mm$). Sample frequency spectrum of the wave obtained from video measurements is shown in Fig. 3. Main frequency of the wave f_0 measured for different liquid metal heights h_0 fits well (see Fig. 4) with the gravity wave one given by formula for two immiscible liquids:

$$f_0 = \frac{1}{L} \sqrt{\frac{g(\rho_1 - \rho_2)}{\frac{\rho_1}{h_1} + \frac{\rho_2}{h_2}}}, \quad (1)$$

where L – horizontal dimension of the box, ρ_1 , ρ_2 are densities and h_1 , h_2 are heights of lower and upper liquid respectively ($h_1 = h_0$ in our notation).

The amplitude of the liquid metal surface elevation is found to depend linearly on the anode current I_0 . This is demonstrated in Fig. 5 for two fixed values of external magnetic field B_0 . One can see that for higher induction of the magnetic field the surface oscillations are growing faster.

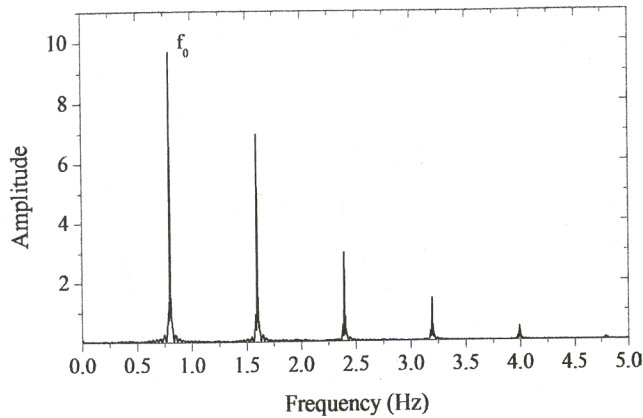


Fig. 3 Frequency spectra of the wave obtained from video measurements at $B_0 = 20 \text{ mT}$, $I_0 = 1 \text{ kA}$, $h_0 = 25 \text{ mm}$; $f_0 = 0.75 \text{ Hz}$.

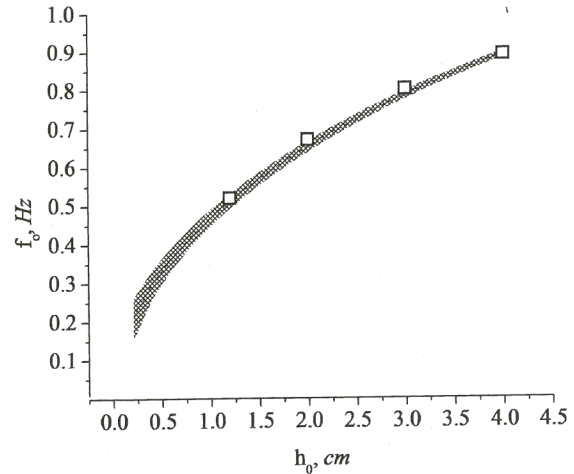


Fig. 4 Dependence of the main wave frequency f_0 on the height of the liquid metal pad h_0 ; shaded area is computed according (1); area width corresponds to the error of height measurement in the experiment (0.5mm); squares – experimental data.

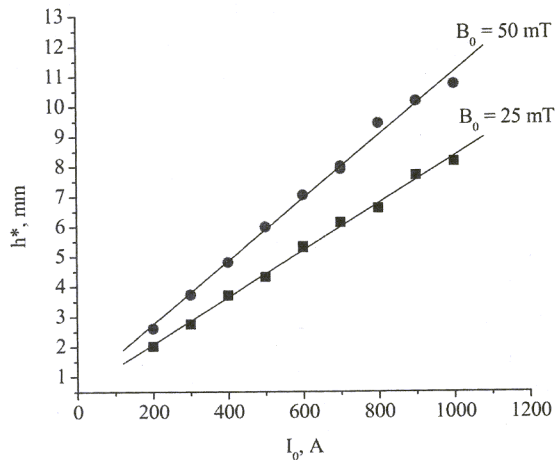


Fig. 5 RMS value of interface fluctuations h^* vs. current I_0 .

threshold of instability is lower for i) lower thickness of the liquid metal layer, h , ii) higher vertical current, I , iii) higher background magnetic field, B_0

Acknowledgments

This work has been performed within the Aluminium Smelter Project No. 2005-3-2723-7 funded by Carbon Trust (UK), Rio Tinto Alcan, Coventry University and University of Warwick. The authors are grateful to the above parties for the financial support.

References

- [1] Sele, T. Instabilities of the metal surface in electrolytic cells. *Light Metals*, 1977, pp 313-322
- [2] Gerbeau, J.-F., Le Bris, C., Lelievre, T. *Mathematical Methods for the Magnetohydrodynamics of Liquid Metals*. Oxford University Press (2006)

Conclusions

The results show that the replacement of an electrolyte layer, which is normally located on top of liquid metal, with a system of vertical electrodes is a viable method to study instabilities relevant to aluminium reduction cells experimentally. This eliminates electrolysis and many other undesired effects associated with it, such as excessively high Joule heating, production of hazardous gases, etc. This also allows to operate with much higher electric currents at room temperature, and thus to study various phenomena related to aluminium reduction cells in a laboratory.

As expected, the results of the experimental study presented here show that instability appears due to interaction of the horizontal currents in the liquid metal layer and the vertical background magnetic field. The